ISSN 0003-701X, Applied Solar Energy, 2022, Vol. 58, No. 6, pp. 800–812. © Allerton Press, Inc., 2022.

SOLAR INSTALLATIONS AND THEIR APPLICATION

A Generic Model for Optimum Tilt Angle of Flat-Plate Solar Harvesters for Middle East and North Africa Region

Yasser F. Nassar[a], *, Ahmad A. Hafez[b], Said Belhaj[c], Samer Y. Alsadi[d], Mohammad J. Abdunnabi[c], Basim Belgasim[c], and Mohamed N. Sbeta[c]

[a] *Mechanical and Renewable Energy, Engineering Department, Faculty of Engineering, Wadi Alshatti University, Brack, Libya*
[b] *Electrical Enginering Department, Faculty of Engineering, Assiut University, Assiut, Egypt*
[c] *Center for Solar Energy Research and Studies, Tripoli, Libya*
[d] *Electrical Engineering Department, Palestine Technical University-Kadoorie, Tulkarm, Palestine*
**e-mail: y.nassar@wau.edu.lu*

Received August 23, 2021; revised November 7, 2021; accepted December 13, 2022

Abstract—The present research proposes a comprehensive model to estimate the optimum annual fixed mode tilt angle (β_{opt}) as a function of all parameters that affect the intensity of solar irradiance incident on a tilted plane such as: latitude ($\varnothing$), diffuse fraction (H_d/H_g) and albedo (ρ_g) by using the weighting functions. It is a useful tool in obtaining a weighted fit when estimating the unknown parameters in a model. The horizontal components of solar irradiation are obtained via SODA database platform based on a reliable-validated hourly time series satellite-derived data for 19 sites on the Middle East and North Africa region. The Klucher anisotropic sky-diffuse transposition model is adopted in order to estimate the global tilted solar irradiance, as it recommended for many sites in MENA region. A polynomial regression model, is proposed to estimate β_{opt} as the product of all the above weighting functions and the latitude as $\beta_{opt} = \varnothing\, W(\varnothing) W\left(\frac{H_d}{H_g}, \rho_g\right)$. The proposed model was validated using several statistical indicators and compared with other results obtained by other researchers for different sky and albedo conditions. The results proved the applicability and reliability of the proposed model, as the R-square index showed that 89% of the considered sites were greater than 0.98, and the MBE index showed that 84% of the locations were less than one. The difference between the results obtained by the propose model and the calculated ones was less than 2% error for all sites except for Sana'a (6%). Moreover, they showed the high potential of the proposed model for use in engineering design, eco-energetic analysis and optimum design processes.

Keywords: optimum tilt angle, weighting function, solar radiation, transposition models, MENA
DOI: 10.3103/S0003701X22060135

ABBREVIATIONS

DNI	Direct normal irradiation, W/m^2
h	Time, h
H_b	Direct beam, W/m^2
H_d	Sky-diffuse, W/m^2
H_t	Global solar radiation incident on an inclined surface, W/m^2
H_g	Global solar radiation incident on a horizontal surface, W/m^2
n	Julian day
R_r	Transposition factor for ground-reflected solar irradiance
R_b	Transposition factor for beam solar irradiance
R_d	Transposition factor for sky-diffuse solar irradiance
W	Weighting function
$\varnothing$	Latitude
β	Solar collector tilt angle
δ	Solar declination angle
θ_i	Solar incident angle
θ_z	Zenith angle
ρ_g	Albedo
ξ	Element
Subscripts	
Opt	Optimum

Ref Reference
Con Condition

1. INTRODUCTION

In addition to the fact that solar energy has become more competitive in the global energy market, it believes that solar energy can play a crucial role in global environmental issues [1].

The technical, environmental and economic feasibility of thermal and electrical solar energy conversion systems has been proved in many MENA's countries. Ramadan and Elistratov analysed the techno-economic feasibility of installing a 300 kW grid-connected solar photovoltaic (PV) plant in Syria [2]. Hafez et al. examined the Technical and Economic Feasibility of Utility-Scale Solar Energy Conversion Systems in Saudi Arabia [3]. Awad et al. proved the enviroeconomic feasibility of rooftop photovoltaic energy system for Assuit University, Egypt [4]. In Palestine [5], Libya [6] and more.

The solar radiation (SR) at the solar collectors is a small fractional of that emitted from the Sun. Thus, solar energy harvesters usually employ different tracking techniques to maximize the captured SR and hence harvested solar power. The intensity of SR reaches its maximum value when it coincides with the verticality of radiation on the surface of the solar collector (i.e. the solar incident angle $\theta_i = 0$). For this reason, designers of solar energy systems tried to tilt the solar collectors to the optimum tilt angle (β_{opt}) to collect the largest amount of SR. Carolina et al. revelled that disinclination by 10° from β_{opt} leads to reduction in energy collection by 1%, and the reduction reaches to 18% for 40° tilt angle [7]. Solar collectors are usually facing the equator and the tilt is fixed to β_{opt} or periodically and manually adjusted. However, to keep the system always at β_{opt}, solar tracking systems should be involved. Nassar indicated that the tracking system would boost SR by around 38% comparing with the fixed ones [8].

For fixed mode flat-plate solar harvesters (PV panels or flat-plate solar heating collectors); the β_{opt} is determined by software tools according to site specific weather data, such as: TMY or satellite-derived data [7]. However, the shortage of meteorological data and the calculation tools in many countries, especially in most of developing countries, force the designers of solar systems to adopt simple generic mathematical models for estimating the optimum tilt angle as a function of minimum quantity of local meteorological data [9].

To calculate the annual optimum tilt angle β_{opt}, two main optimization criteria could be considered. The first is the maximum load covered by the solar system, which is usually appropriate for small solar applications [10]. The second is maximum the total annual solar irradiance incident on the tilted solar collector, which is usually adopted for large solar systems [11].

Evolutionary approaches are advised for calculating the optimum tilt angle [12–16]. Artificial neural network [12], as the literature claims, has the advantage of good global searching capability and learning the approximate optimal solution without the gradient information of the error functions. Neural Network however, has its own limitations. It is easy to fall into local minimum and sometimes hard to adjust the architecture [15]. Particle swarm optimization algorithm [13] has high accuracy solutions and stable convergence criteria than other stochastic methods. The major drawback of PSO, like in other heuristic optimization techniques, is lacking a solid mathematical foundation. Particle swarm requires also a relatively longer computation time than the mathematical approaches [16]. Genetic algorithm [14] has the capability to handle multiple solution search spaces and solve the given problem in such an environment. Moreover, genetic algorithms are less complex and more straightforward compared to other algorithms. In addition, genetic algorithms are easier to be transferred and applied in different platforms, thereby increasing its flexibility. The main disadvantage of genetic algorithm involves computation efficiency and convergence [17].

The knowledge of the exact transposition model is very important for calculate the optimum tilt angle of solar collectors [18]. Yadav and Chandel experimentally tested the validation of six transposition models under outdoor conditions. They found that the Liu and Jordan model has the best estimation for the optimum tilt angle [19]. Hua et al. estimated the optimum tilt angle of solar panels for a city in northwest China with three types of transposition models, Liu and Jordan, Hay and Klein and Theilacker model. The study found that the calculated yearly optimum tilt angles by three models are close among each other [20]. While, Kumar et al., experimentally studied the effect of tilt angles on the behaviour of air heating solar collector for Telangana city in India. They found that the maximum heat gain by the fluid at 25° tilt angle is approximately 3 times higher at 60° tilt angle [21].

Numerous studies have attempted to obtain the optimum annual tilt angle (β_{opt}) for different locations as a function of latitude (∅) [22–24], weather conditions [25], the characteristics of energy demand [26–28], increasing solar radiation incident on the surface of flat-plate solar collector [29], and to Maximize electricity generation [30]. However, there is lack in the literature regarding the studies that could express β_{opt} as a multi-variable function of latitude and other local parameters. The literature as [31] determines the parameters that affect the determination of β_{opt} in addition to latitude. They as claimed in [31] are the site altitude, temperature, humidity, clearness index, albedo and/or land-use area [31]. Hafez et al.

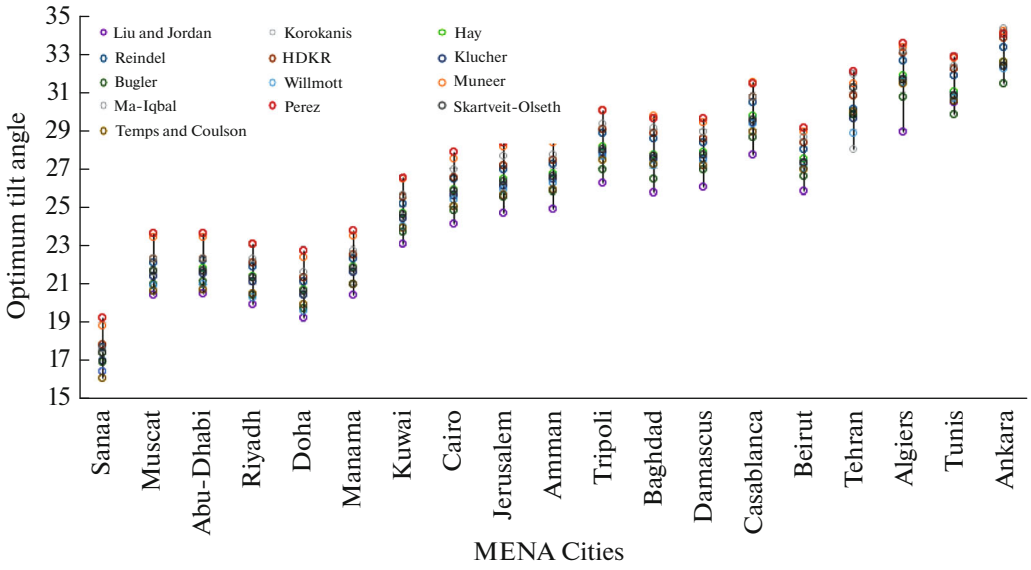

Fig. 1. Optimum tilt angles of solar collectors for MERNA cities according to all transposition models.

reviewed and tabulated the optimum tilt angle correlations in solar energy applications for many countries [22]. Danandeh and Mousavi provided the main approaches for determining the optimum tilt angle [23]. Many researchers have attempted to determine the optimum tilt angle for many locations, for example: Cairo and Quina -Egypt [24, 25] Kumasi-Ghana [26], Veracruz-Mexico [27], Sabang -Indonesia [28], Kano-Nigeria [31], Toronto-Canada [32], Ontario-Canada [33], Settat-Morocco [34], Daegu-South Korea [35], Tabass-Iran [36], Gaza-Palestine [14], Kuwait- Kuwait [37], Muscat-Oman [38], Doha – Qatar [39], Riyadh – Saudi [40], Abu Dhobi – UAE [41], Algiers—Algeria [42]. Other researchers attempted to derive general expressions for large zones or even for any location around the world, such as: Syria [43], Palestine [44], Algeria [45], Turkey [46], Saudi Arabia [47, 48], the Mediterranean region [11], mid and high latitudes [12], desert environment [49], northern hemisphere [50], and for all the world [51, 52].

Despite the large research efforts in this area, erroneous tilt angles are still to be found in many solar collector installations [53]. Most of these studies derived linear expressions in the form of ($\beta_{opt} = \varnothing \pm$ value) as a function of latitude for fixed annual optimum tilt angle [51], and ($\beta_{opt} = \varnothing \pm \delta$) as a function of latitude and solar declination angle for monthly tilt angle adjustment [52]. However, these studies ignored weather characteristics (namely diffuse to global solar radiation ratio) as well as location characteristics (namely ground-albedo). The weather and location characteristics are considered for the proposed model in this research as well as the conventional parameters.

In conclusion, the tilt angle of solar harvesters can be considered the critical variable in the design of thermal and electrical solar systems. Identification of β_{opt} for a certain location needs to obtain the following solar irradiance components: global horizontal H_g, global tilted H_t, horizontal sky-diffuse H_d, and albedo ρ_g. These essential data can be obtained from weather stations, Satellite-derived data, or using validated empirical equations for a site. Subsequently, an adequate transposition model must be selected in order to account for all three components at the tilt angle. Nassar et al. evaluated and compared the performance of 24 distinct transposition models [54].

Figure 1 illustrates the Optimum tilt angles of solar collectors for MENA cities according to different transposition models. Figure 2 shows the sensitivity of the locations to the specific transposition model.

Figure 1 shows that optimum tilt angle is less dependent on the transposition model, as the maximum deviation of optimum tilt angle is not exceeding than 5 deg. This is shown clearly in Fig. 2, where the rate of deviation of different transposition models from the average optimum tilt angle is illustrated in bubbles chart. Figure 2 shows that Hay and Klucher models are the most accurate, but the Klucher model was adopted here in this research due to its simplicity and lower requirements than Hay's model.

In this research, all the parameters that affected the identification of the optimum tilt angle of a solar collector ($\varnothing$, $\frac{H_d}{H_g}$ and ρ_g) are considered. Then, weighting function concept is used for developing a regression model that allows computation of the optimum tilt angle in any location at the MENA region. The proposed optimum tilt angle could be used for instantaneous adjusting of the solar collectors in MENA such

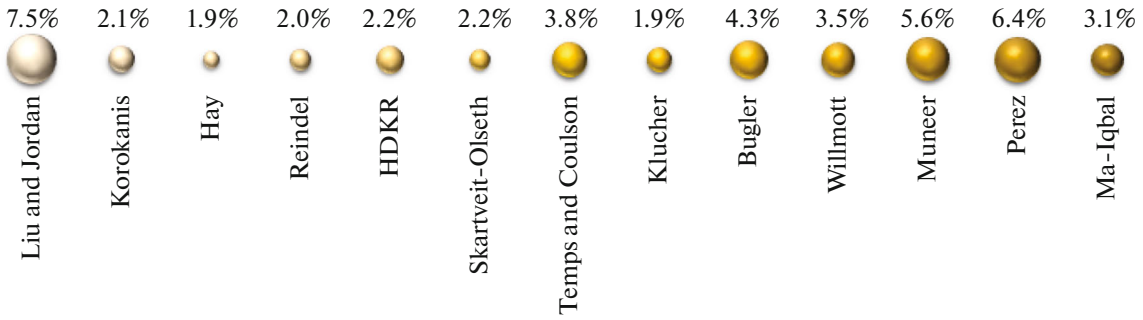

Fig. 2. Deviation percentage of each model from the average tilt angle.

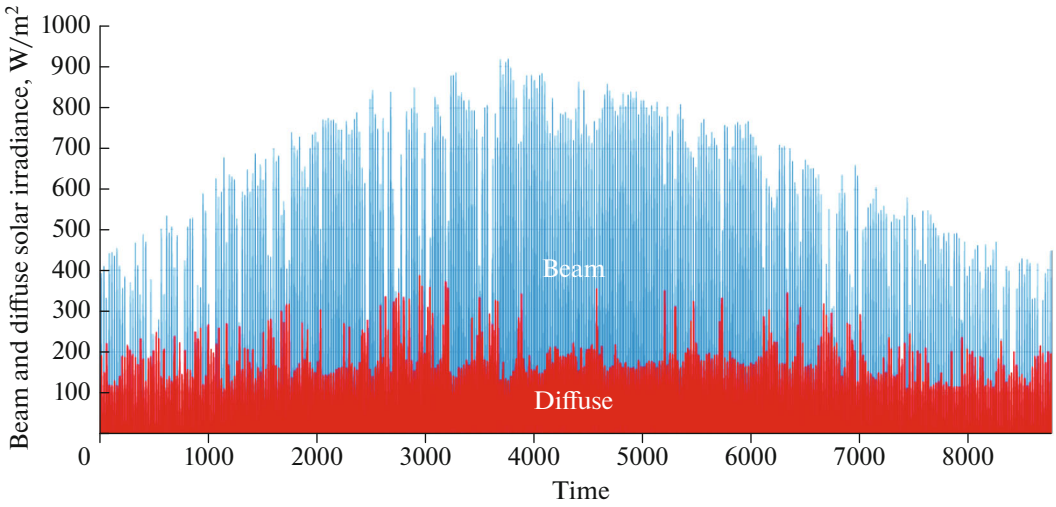

Fig. 3. Hourly horizontal beam and diffuse solar irradiance for Tripoli (32.815° N, 13.439° E).

that they captured the maximum SR. This would optimize the solar energy projects. The validity of the proposed model; is assessed via several statistical model performance indicators. The main contributions of this article could be:

• Proposing simple and generic approach for estimating the optimum tilt angle of MENA region under different climatological and operating conditions.

• Validating the proposed model via different statistical indicators.

2. DATA AND METHODOLOGY

2.1. Data

The data used in this research was hourly time series solar radiation data from Soda service derived from satellite MERRA-2/NASA, for the period of 2004-02-01 to 2006-12-31 (http://www.soda-pro.com/web-services/radiation/helioclim-3-archives-for-free). The data included global inclined (H_t), global horizontal radiation (H_g), diffuse horizontal radiation (H_d), direct normal radiation (DNI), extra-terrestrial radiation, air temperature, relative humidity, pressure, wind speed, wind direction and snowfall.

Solar irradiance data of Tripoli (32.815° N, 13.439° E)-Libya for a year in the period of 2019–2020 are used for deriving the proposed model (Fig. 3). These data are obtained from bulletin of the centre of Solar Energy Research and Studies, Tripoli-Libya.

Figure 3 confirms the feasibility of solar energy harvesting and hence optimum tilt angle for maximizing the harvested energy. Moreover, Tripoli-Libya enjoys nearly moderate temperature throughout the year (Fig. 4), which increases its potential for different types of solar energy project.

Figure 4 again confirms the visibility and potential of solar energy project particularly PV for the site under concern. The average temperature is 23°C, which is lower than the normal operating conditions for most of commercial PV modules [55–58].

This boost the output power and hence the economic value of the project.

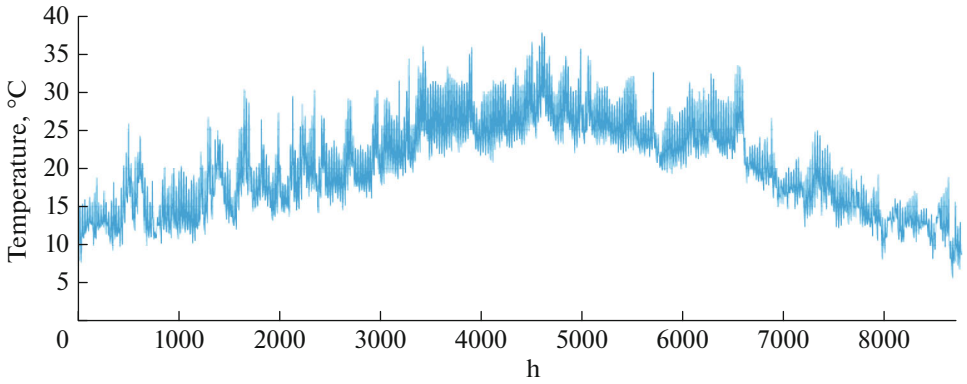

Fig. 4. Hourly air temperature for Tripoli City-Libya.

2.2. Methodology

The proposed optimum tilt angle is determined via the following steps.

(2.2.1) Global (H_g) and sky-diffuse (H_d) solar radiation are identified.

(2.2.2) Global tilted solar irradiance (H_t) on the inclined surface of a solar collector was then calculated.

(2.2.3) Optimum tilt angle for a solar collector β_{opt} is determined for specific locations.

(2.2.4) Generic optimum tilt angle (β_{opt}) for all sky $\left(0 \le \frac{H_d}{H_g} \le 1\right)$, ground $(0 \le \rho_g \le 1)$ conditions and for anonymous site on Earth $(0 \le \varnothing \le 90)$.

2.2.1. Global solar radiation, H_g. Global solar radiation, H_t incident on an inclined surface requires data for global horizontal, H_g, and sky-diffuse (H_d). H_g has two components: direct beam (H_b) and sky-diffuse, H_d, radiation, as given by [7, 8]:

$$H_g = H_b + H_d, \tag{1}$$

H_b, H_d could be obtained in the form of recorded time series solar data from meteorological stations, or from modelled databases based on satellite imagery analysis.

2.2.2. Global tilted solar irradiance, H_t. Transposition models are used to calculate H_t from H_g and its components. Thus, global solar irradiance for a tilted surface, H_t, at a tilt angle (β) from the horizontal is given by [7, 8]:

$$H_t = H_b R_b + H_d R_d + H_g R_r. \tag{2}$$

Equation (2) could be rewritten in the form of diffuse to global solar radiation ratio:

$$\frac{H_t}{H_g} = \left(1 - \frac{H_d}{H_g}\right) R_b + \frac{H_d}{H_g} R_d + R_r. \tag{3}$$

The transposition factor (R_b) is represented as a function of Sun's location in the sky and the geometrical parameters of the tilted surface by [7, 8],

$$R_b = \max\left(0, \frac{\cos\theta_i}{\cos\theta_z}\right), \tag{4}$$

where θ_i, θ_z are solar angle of incidence and zenith angle respectively. Similarly, R_r is the transposition factor for ground-reflected solar irradiance and it is given by:

$$R_r = \rho_g \frac{1 - \cos\beta}{2}, \tag{5}$$

where ρ_g is the ground reflectivity—albedo. The value of ρ_g is a positive value less than one according to the reflectivity of the ground surrounding the collector. ρ_g is usually assumed a constant 0.2 [59]. However, some transposition models as Sandia use variable value for ρ_g [60].

The sky-diffuse radiation is due to the scattering of solar radiation by the different elements of the atmosphere (air molecules, tiny water droplets, ice crystals, or aerosols), giving a non-uniform distribution throughout the sky dome. However, models such as Liu and Jordan, Korokanis, Jimenez and Castro, Tian and Badescu consider diffuse radiation as being uniform or isotropic [7]. Other models are concerning with the forward scattering of solar radiation concentrated around the sun known as circumsolar diffuse. Another irradiance component, which is horizon brightening concentrated irradiance, usually is pronounced in clear skies. The anisotropic models such as Bugler, Temps-Coulson, Steven and Unsworth, Hay, Klucher, Willmot, Ma-Iqbal, Skartveit-Olseth, and Perez include circumsolar diffuse and horizon brightening [7]. A recent study indicates that the Klucher

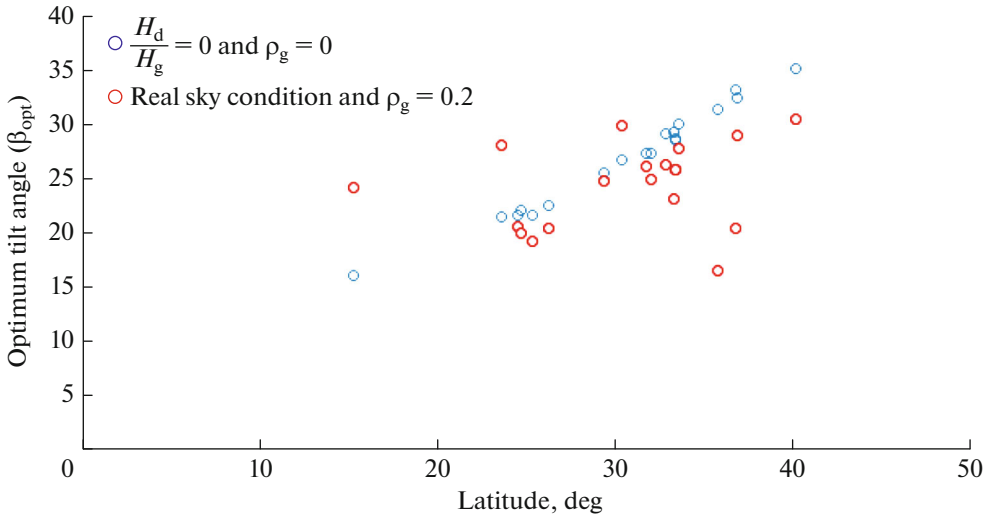

Fig. 5. Optimum tilt angle vs. latitude for real sky (red circle) and $\rho_g = 0$, $\frac{H_d}{H_g} = 0$ (blue circle).

anisotropic transposition model is the most accurate for many sites in MENA region, and for this reason it was used for estimating the global inclined solar irradiance components [61], as,

$$R_d = \left(\cos^2\frac{\beta}{2}\right)\left(1 + f_K \cos^2\theta_i \sin^3\theta_z\right) \times \left(1 + f_K \sin^3\frac{\beta}{2}\right), \quad (6)$$

where, $f_K = 1 - \left(\frac{H_d}{H_g}\right)^2$.

2.2.3. Optimum tilt angle a solar collector β_{opt}. The optimum tilt angle β_{opt} is a multivariable function. Therefore, an iterative search algorithm used to determine the optimum tilt angle for given input conditions. This is to identify the characteristics and relativeness of different variables for β_{opt}. The search algorithm requires, however, a sky-diffuse transposition model. The search algorithm and transposition model were coded in higher level machine language. Then, they are wrapped in a Dynamic Link Library (DLL), using MS-Excel as the front-end to interact with the user. MS-Excel is used due to its simplicity and popularity. The software tool was then used to establish the optimum tilt angle (β_{opt}) for given locations, under all weather and ground conditions ($0 \le \rho_g \le 1$ and $0 \le \frac{H_d}{H_g} \le 1$). The obtained results were plotted in Fig. 5.

Figure 5 shows that optimum tilt angle for the scenario of $\rho_g = 0$, $\frac{H_d}{H_g} = 0$ follows geometrical shape. Thus a suitable regression function could be obtained for this case. However, for real sky andurealbedo conditions, optimum tilt angle follows a random distribution, which could not easily modelled by a mathematical formula.

2.2.4. Proposed model of optimum tilt angle. The general expression for the optimum tilt angle for any latitude, all sky conditions, and all albedo values, is the product of all the above weighting functions and the latitude:

$$\beta_{opt}\left(\varnothing, \rho_g, \frac{H_d}{H_g}\right) = \varnothing\, W(\varnothing) W\left(\frac{H_d}{H_g}, \rho_g\right), \quad (7)$$

where $W(\xi)$ is weighting function. The weighting function is a mathematical tool used to mathematically express the significance of the different variables. It is a useful tool in obtaining a weighted fit when estimating the unknown parameters in a model [62]. The weighting function $W(\xi)$ is defined by,

$$W(\xi) = 1 + f(\xi);$$
$$f(\xi) = \left.\frac{\Delta\xi}{\xi_{ref}}\right|_{con} \quad \text{for one group;} \quad (8)$$
$$f(\xi) = \left.\frac{1}{n}\sum_{i=1}^{n}\frac{\Delta\xi_i}{\xi_{i,ref}}\right|_{i,con} \quad \text{for } n \text{ groups,}$$

where ξ represents the element under consideration. The weighting function W could be single or multiple variable. *f* represents the regression function for each element. The subscripts *ref* and *con* refer to the reference point and the conditions at which the optimum tilt angle is calculated. *n* is the number of groups.

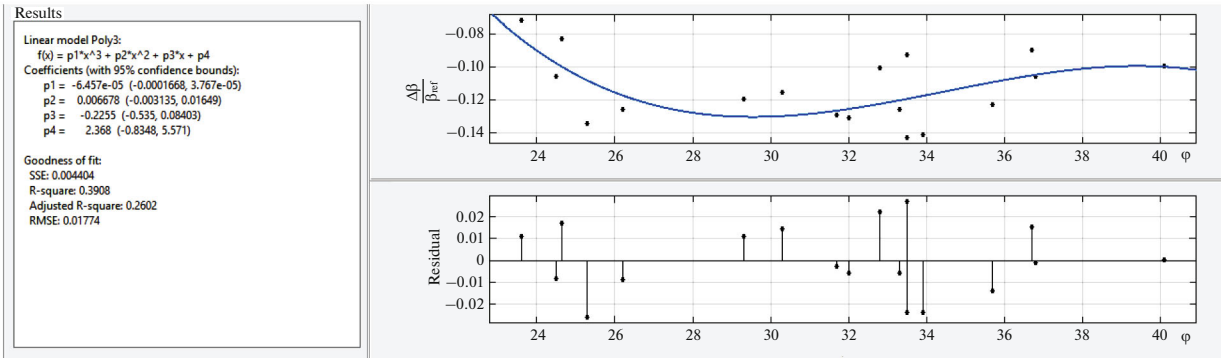

Fig. 6. Relationship between $\left.\frac{\Delta\beta(\varnothing)}{\beta_{ref}}\right|_{\rho_g=0,\frac{H_d}{H_g}=0}$ and $\varnothing$.

2.2.4.1. Latitude regression weighting function $W(\varnothing)$. The reference optimum angle for $W(\varnothing)$ was chosen equal to the latitude angle (i.e. $\beta_{ref} = \varnothing$). The procedure commences with establishing the optimum tilt angle for the considered locations at the conditions $\rho_g = 0$ and $\frac{H_d}{H_g} = 0$, applying (1) to (6) for all tilt angles $0 \le \beta \le 90$ at 0.1° resolution to determine β_{opt}, where the total annual tilted surface global solar radiation is at its peak. After obtaining $\beta_{opt}(\phi)_{\rho_g=0,\frac{H_d}{H_g}=0}$, the term $\left.\frac{\Delta\beta(\varnothing)}{\beta_{ref}}\right|_{\rho_g=0,\frac{H_d}{H_g}=0}$ was calculated from:

$$\left.\frac{\Delta\beta(\varnothing)}{\beta_{ref}}\right|_{\rho_g=0,\frac{H_d}{H_g}=0} = \left.\frac{\beta_{opt}(\varnothing)-\beta_{ref}}{\beta_{ref}}\right|_{\rho_g=0,\frac{H_d}{H_g}=0} = \left.\frac{\beta_{opt}(\varnothing)-\varnothing}{\varnothing}\right|_{\rho_g=0,\frac{H_d}{H_g}=0}, \quad (9)$$

where $\beta_{opt}(\varnothing)$ is the observed optimum tilt angle for the conditions $\rho_g = 0$ and $\frac{H_d}{H_g} = 0$, and $\varnothing$ is the latitude of the location. Figure 6 depicts the relationship between the term $\left.\frac{\Delta\beta(\varnothing)}{\beta_{ref}}\right|_{\rho_g=0,\frac{H_d}{H_g}=0}$ and latitude ($\varnothing$), as well as the mathematical regression model and the residuals.

The polynomial regression $f(\varnothing)$ that appears in Fig. 6 represents the curve fitting of $\left.\frac{\Delta\beta(\varnothing)}{\beta_{ref}}\right|_{\rho_g=0,\frac{H_d}{H_g}=0}$ verses latitude $\varnothing$, giving the expression for the latitude weighting function $W(\varnothing)$:

$$W(\varnothing) = (1 + f(\varnothing)) = \left(-6.3e^{-05}\varnothing^3 + 6.678e^{-03}\varnothing^2 - 0.224\varnothing + 3.26\right) \quad (10)$$

and the predicted optimum tilt angle:

$$\beta_{opt}(\varnothing) = \varnothing W(\varnothing). \quad (11)$$

The obtained results are tabulated in Table 1.

2.2.4.2. Diffuse to global solar radiation ratio and albedo square regression weighting function $W\left(\frac{H_d}{H_g}, \rho_g\right)$. The terms $\left.\frac{\Delta\beta(\rho_g)}{\beta_{ref}}\right|_{\frac{H_d}{H_g}=0}$ and $\left.\frac{\Delta\beta\left(\frac{H_d}{H_g}\right)}{\beta_{ref}}\right|_{\rho_g=0}$ were calculated as $\left.\frac{\Delta\beta(\varnothing)}{\beta_{ref}}\right|_{\rho_g=0,\frac{H_d}{H_g}=0}$. With two independent variables, multiple linear regression 3D analysis was used to model the relationship representing the weighting functions for albedo and diffuse to global solar radiation ratio. The value of $\frac{\Delta\beta\left(\frac{H_d}{H_g},\rho_g\right)}{\beta_{ref}}$ was calculated for each site and then the average value was obtained using (7). The reference tilt angle was chosen as $\beta_{\left(\rho_g=0,\ \frac{H_d}{H_g}=0\right)}$ and the term $\frac{\Delta\beta\left(\frac{H_d}{H_g},\rho_g\right)}{\beta_{ref}}$ for each site (i) was calculated using the equations:

$$\left.\frac{\Delta\beta\left(\frac{H_d}{H_g},\rho_g\right)}{\beta_{ref}}\right|_i = \left.\frac{\beta_{opt}\left(\frac{H_d}{H_g},\rho_g\right)-\beta_{\left(\rho_g=0,\ \frac{H_d}{H_g}=0\right)}}{\beta_{\left(\rho_g=0,\ \frac{H_d}{H_g}=0\right)}}\right|_i, \quad (12)$$

Table 1. β_{opt} and $\frac{\Delta\beta(\varnothing)}{\beta_{ref}}$ calculated at $\beta_{ref} = \varnothing$, for conditions $\rho_g = 0$ and $\frac{H_d}{H_g} = 0$

City	Latitude (∅)	Observed $\beta_{opt}(\varnothing)\Big\|_{\left(\rho_g=0,\ \frac{H_d}{H_g}=0\right)}$	Value of $\frac{\Delta\beta(\varnothing)}{\beta_{ref}}\Big\|_{\left(\rho_g=0,\ \frac{H_d}{H_g}=0\right)}$	Predicted $\beta_{opt}(\varnothing)$
Sanaa	15.3	15.9	0.035831	19.10
Muscat	23.6	21.9	−0.07203	21.64
Abu-Dhabi	24.5	21.9	−0.10612	22.11
Riyadh	24.65	22.6	−0.08316	22.19
Doha	25.3	21.9	−0.13439	22.57
Manama	26.2	22.9	−0.12595	23.13
Kuwait	29.3	25.8	−0.11945	25.49
Cairo	30.3	26.8	−0.11551	26.37
Jerusalem	31.7	27.6	−0.12934	27.69
Amman	32	27.8	−0.13125	27.98
Tripoli	32.8	29.5	−0.10061	28.78
Baghdad	33.3	29.1	−0.12613	29.29
Casablanca	33.5	30.4	−0.09254	29.50
Damascus	33.5	28.7	−0.14328	29.50
Beirut	33.9	29.1	−0.14159	29.91
Tehran	35.7	31.3	−0.12325	31.80
Algiers	36.7	33.4	−0.08992	32.84
Tunis	36.8	32.9	−0.10598	32.95
Ankara	40.1	36.1	−0.09975	36.11

$$\frac{\Delta\beta\left(\frac{H_d}{H_g},\rho_g\right)}{\beta_{ref}} = \frac{1}{n}\sum_{i=1}^{n}\left.\frac{\beta_{opt}\left(\frac{H_d}{H_g},\rho_g\right) - \beta_{\left(\rho_g=0,\ \frac{H_d}{H_g}=0\right)}}{\beta_{\left(\rho_g=0,\ \frac{H_d}{H_g}=0\right)}}\right|_i. \quad (13)$$

Surface fitting was performed using the curve fitting toolbox in MatLab software. The obtained results were plotted in Fig. 7.

The best fitting was found to be of a cubic order polynomial, having R^2 indicator a high 0.997.

The corresponding weighting function is expressed as a function of both ρ_g and $\frac{H_d}{H_g}$:

$$\begin{aligned} W\left(\frac{H_d}{H_g},\rho_g\right) &= 0.993 - 0.7784\left(\frac{H_d}{H_g}\right) \\ &+ 0.7989\rho_g + 1.011\left(\frac{H_d}{H_g}\right)^2 - 0.2082\left(\frac{H_d}{H_g}\right)\rho_g \\ &- 0.8113\rho_g^2 - 1.271\left(\frac{H_d}{H_g}\right)^3 - 0.7213\left(\frac{H_d}{H_g}\right)^2\rho_g \\ &+ 1.204\left(\frac{H_d}{H_g}\right)\rho_g^2 + 0.7537\rho_g^3. \end{aligned} \quad (14)$$

3. STATISTICAL ASSESSMENTS OF PROPOSED MODEL

The statistical indicators Root Mean Square Error (RMSE), Mean Bias Error (MBE) and R-Square were used to assess the goodness of fit of the proposed model [63, 64]. This serves to determine the reliability and accuracy of the proposed model, particularly for the applicable conditions $0 \le \rho_g \le 0.7$ and $0.1 \le \frac{H_d}{H_g} \le 0.8$.

3.1. RMSE

RMSE is alternatively defined as fit standard error and the standard error of regression. It is an estimate of the standard deviation of the random component in the data, and is defined as:

$$\mathrm{RMSE} = \left[\frac{1}{n}\sum_{i=1}^{n}\left(\beta_{i,p} - \beta_{i,c}\right)^2\right]^{1/2}. \quad (15)$$

A value closer to 0 indicates that the model has a smaller random error component and that it produces more accurate predictions.

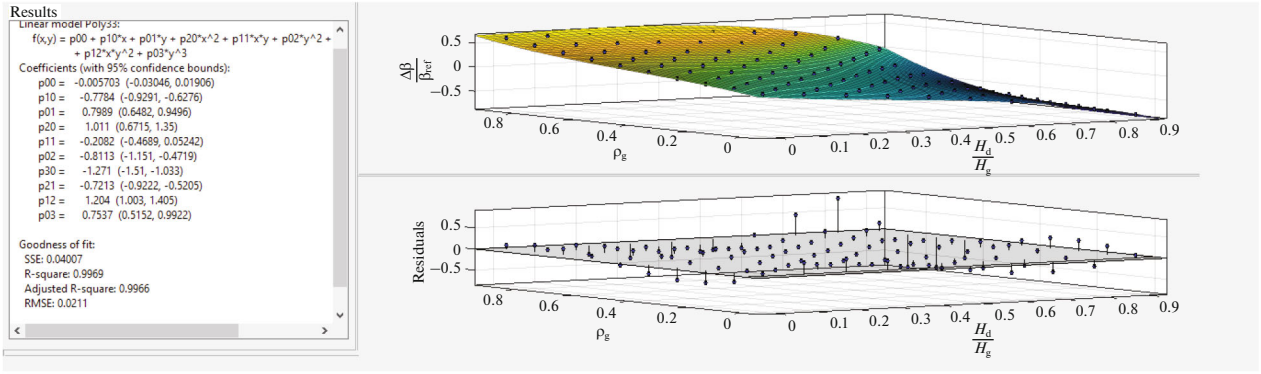

Fig. 7. Surface curve fitting of $\frac{\Delta\beta}{\beta_{ref}}$ as a function of ρ_g, $\frac{H_d}{H_g}$ and polynomial regression.

3.2. MBE

The MBE provide information on the long-term performance of a model. A positive value gives the average amount of over-estimation in the estimated values and vice versa [54]:

$$\text{MBE} = \frac{1}{n}\sum_{i=1}^{n}(\beta_{i,p} - \beta_{i,c}). \quad (16)$$

Smaller absolute values indicate that the model produces more accurate prediction.

3.3. R-Square

R-square measures the effectiveness of the data interpretation. It is also the square of the correlation between the response values and the predicted response values. R-square is also called the square of the multiple correlation coefficient and the coefficient of multiple determination. It is defined as:

$$R\text{-square} = 1 - \frac{\sum_{i=1}^{n}(\beta_{i,p} - \beta_{i,c})^2}{\sum_{i=1}^{n}(\beta_{i,c} - \beta_{\text{av},c})^2}, \quad (17)$$

where $\beta_{\text{av},c}$ is the mean of the calculated optimum tilt angle. *R*-square values close to 1.0 indicate better model performance.

4. RESULTS AND DISCUSSIONS

The results obtained by applying the general expression for the optimum tilt angle Eq. (14) for different latitudes, sky conditions, and albedo values, is plotted versus the reported results, Fig. 8.

Figure 8 shows that the reported and (17) results are correlated. They are nearly identical. This clearly demonstrates the ability of the proposed model to predict the optimum tilt angle for the MENA region, showing strong correlation between the observed and predicted optimum angles for latitudes above the Tropic of Cancer.

Figure 8 also shows that for Sanaa at latitude 15.3° there is around 6% difference, which may return to geological characteristics of Sanaa.

The values of the statistical indicators RMSE, MBE and R-Square for different sites in MENA region under different sky and albedo conditions are shown in Table 2.

Table 2 confirms the reliability and validity of the proposed optimum tilt angle model. R-square for the different sites in MENA region is close to unity except for Sanaa, which correlates with Fig. 7. The difference in the statistical indicators could be attributed to sky and albedo conditions. The proposed optimum tilt angle model produces the most accurate results for Tripoli, Riyadh and Cairo. This could return to that they have very close longitude locations.

5. CONCLUSIONS

The optimum tilt angle for fixed solar harvesters has significant contribution in maximizing the harvest energy and hence economics of the solar projects. However, the reported optimum tilt angles in literature either are not accurate or require complicated calculations. Therefore, the article proposes a simple procedure for deriving a formula for optimum tilt angle for MENA region. The proposed equation is generic, thus it is applicable for different locations, sky conditions and albedo. The proposed optimum tilt formula is derived from the different components of the solar radiation. These components are obtained from SODA database platform based on a reliable-validated hourly time series satellite-derived data.

RMSE, MBE and R-Square are statistical tools are used to assess the viability and quality of the proposed model. Around 19 different cities in the MENA region

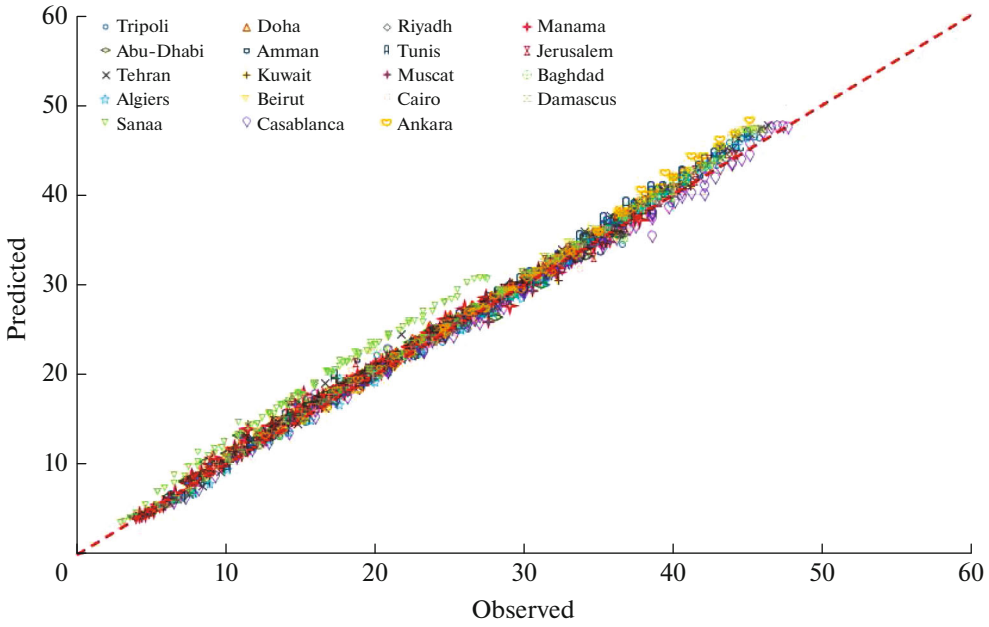

Fig. 8. Comparison between reported and predicted fixed annual optimum tilt angle.

are tested and the results of the proposed model are compared with the calculated.

The results showed that the proposed model efficiently could calculate the optimum tilt angle with high accuracy. Moreover, the simplicity of the produced formula allows its application for not only fixed but for moving solar harvesters as well.

Table 2. Performance of proposed model

City	MBE	*R*-square	RMSE
Tripoli	0.018	0.99	0.91
Doha	0.86	0.98	1.26
Riyadh	0.21	0.99	0.86
Ankara	1.07	0.96	1.53
Manama	0.63	0.98	1.09
Abu-Dhabi	0.45	0.98	1.07
Amman	0.68	0.99	1.12
Tunis	1.02	0.98	1.45
Jerusalem	0.54	0.99	1.04
Tehran	0.81	0.99	1.24
Kuwait	0.26	0.99	0.89
Muscat	0.19	0.99	0.86
Baghdad	0.45	0.99	1.01
Algiers	0.46	0.99	1.20
Beirut	0.95	0.98	1.28
Cairo	–0.01	0.99	0.88
Damascus	0.87	0.99	1.25
Sanaa	2.53	0.82	2.60
Casablanca	–0.45	0.99	1.14

FUNDING

This research received no external funding.

CONFLICT OF INTEREST

The authors declare that they have no conflicts of interest.

DATA AVAILABILITY

The data that support the findings of this study are available within the article and its supplementary material.

REFERENCES

1. Nassar, Y., Alsadi, S., El-Khozondar, H., Ismail, M., Al-Maghalseh, M., Khatib, T., Saed, J., Mushtaha, M., and Djeraf, T., Design of an isolated renewable hybrid energy system: A case study, *Mater. Renewable Sustainable Energy,* 2022, vol. 11, pp. 225–240. https://doi.org/10.1007/s40243-022-00216-1
2. Ramadan, A. and Elistratov, V., Techno-economic evaluation of a grid-connected solar PV plant in Syria, *Appl. Sol. Energy,* 2019, vol. 55, pp. 174–188. https://doi.org/10.3103/S0003701X1903006X
3. Hafez, A., Nassar, Y., Hammdan, M., and Alsadi, S., Technical and economic feasibility of utility-scale solar energy conversion systems in Saudi Arabia, *Iran. J. Sci. Technol., Trans. Electr. Eng.,* 2020, vol. 44, pp. 213–225. https://doi.org/10.1007/s40998-019-00233-3

4. Awad, H., Nassar, Y., Hafez, A., Sherbiny, M., and Ali, A., Optimal design and economic feasibility of rooftop photovoltaic energy system for Assuit University, Egypt, *Ain Shams Eng. J.,* 2022, vol. 13, no. 3, pp. 810–816. https://doi.org/10.1016/j.asej.2021.09.026
5. Nassar, Y. and Alsadi, S., Economical and environmental feasibility of the renewable energy as a sustainable solution for the electricity crisis in the Gaza Strip, *Int. J. Eng. Res. Dev.,* 2016, vol. 12, no. 3, pp. 35–44. https://www.researchgate.net/publication/301328870
6. Nassar, Y., Abdunnabi, M., Sbeta, M., Hafez, A., Amer, K., Ahmed, A., and Belgasim, B., Dynamic analysis and sizing optimization of a pumped hydroelectric storage-integrated hybrid PV/wind system: A case study, *Energy Convers. Manage.,* 2021, vol. 229, p. 113744. https://doi.org/10.1016/j.enconman.2020.113744
7. Duffie, J.A. and Beckman, W.A., *Solar Engineering of Thermal Processes,* New York: Wiley, 2013. https://doi.org/10.1002/9781118671603
8. Nassar, Y.F., *Solar energy engineering active applications*, Sebha University, Libya, 2006.
9. Omar, A. and Mahmoud, M., Grid connected PV-home systems in Palestine: A review on technical performance, effects and economic feasibility, *Renewable Sustainable Energy Rev.,* 2018, vol. 82, pp. 2490–2497. https://doi.org/10.1016/j.rser.2017.09.008
10. Tian, C., The Sun's apparent position and the optimal tilt angle of a solar collector in the northern hemisphere, *Sol. Energy,* 2009, vol. 83, pp. 1274–1284. https://doi.org/10.1016/j.solener.2009.02.009
11. Darhmaoui, H. and Lahjouji, D., Latitude based model for tilt angle optimization for solar collectors in the Mediterranean region, *Energy Procedia,* 2013, vol. 42, pp. 426–435. https://doi.org/10.1016/j.egypro.2013.11.043
12. Alsadi, S., Nassar, Y., and Amer, K., General polynomial for optimizing the tilt angle of flat solar energy harvesters based on ASHRAE clear sky model in mid and high latitudes, *Energy Power,* 2016, vol. 6, no. 2, pp. 29–38. https://doi.org/10.5923/j.ep.20160602.01
13. Al-Nuaimi, A. and Barrou, N., Modeling global, direct, diffuse solar radiation and the optimum tilt angle in some selected Libyan cities, *Int. J. Appl. Sci.,* 2019, vol. 1, no. 1. https://doi.org/10.53555/ephas.v1i1.1333
14. Alsadi, S. and Nassar, Y., Energy demand based procedure for tilt angle optimization of solar collectors in developing countries, *J. Fund. Renewable Energy Appl.,* 2019, vol. 7, p. 225. https://doi.org/10.4172/20904541.1000225
15. Elwani, A., Dekam, E., and Agha, K., A normalized mathematical model for optimum tilt angles based on the desired solar fraction, *Int. J. Recent Dev. Eng. Technol.,* 2019, vol. 8, no. 1. https://www.ijrdet.com/files/Volume8Issue1/IJRDET_0119_01.pdf.
16. Shariah, A., Al-Akhras, M., and Al-Omari, I., Optimizing the tilt angle of solar collectors, *Renewable Energy,* 2020, vol. 26, pp. 587–598.
17. Kadav, A. and Chandel, S., Tilt angle optimization to maximize incident solar radiation: A review, *Renewable Sustainable Energy Rev.,* 2013, vol. 23, pp. 503–513. https://doi.org/10.1016/j.rser.2013.02.027
18. Nassar, F., Abuhamoud, N., Miskeen, G., El-Khozondar, H., Alsadi, S., and Ahwidi, O., Investigating the applicability of horizontal to tilted sky-diffuse solar irradiation transposition models for key Libyan cities, *2022 IEEE 2nd International Maghreb Meeting of the Conference on Sciences and Techniques of Automatic Control and Computer Engineering (MI-STA 2022),* Sabratha, Libya, May 23–25, 2022. https://doi.org/10.1109/MI-STA54861.2022.9837500
19. Yadav, P. and Chandel, S., Comparative analysis of diffused solar radiation models for optimum tilt angle determination for Indian locations, *Appl. Sol. Energy,* 2014, 50, pp. 53–59. https://doi.org/10.3103/S0003701X14010137
20. Hua, Y., He, W., and Liu, P., Optimum tilt angles of solar panels: A case study for Gansu Province, Northwest China, *Appl. Sol. Energy,* 2020, vol. 56, pp. 388–396. https://doi.org/10.3103/S0003701X20050060
21. Kumar, S., Sridhar, K., and Kumar, G., Heat transfer analysis of solar air heating system for different tilt angles, *Appl. Sol. Energy,* 2018, vol. 54, pp. 17–22. https://doi.org/10.3103/S0003701X18010085
22. Hafez, A., Soliman, A., El-Metwally, K., and Islam, I., Tilt and azimuth angles in solar energy application—A review, *Renewable Sustainable Energy Rev.,* 2017, vol. 77, pp. 147–168. https://doi.org/10.1016/j.rser.2017.03.131
23. Danandeh, M. and Mousavi, S., Solar irradiance estimation models and optimum tilt angle approaches: A comparative study, *Renewable Sustainable Energy Rev.,* 2018, vol. 92, pp. 319–330. https://doi.org/10.1016/j.rser.2018.05.004
24. Hegazy, A., Estimation of optimum tilt angles for solar collector and gained energy at Cairo, Egypt, *Int. J. Innovative Sci., Eng. Technol.,* 2019, vol. 6, no. 5, pp. 249–258. https://ijiset.com/vol6/v6s5/IJISET_V6_I5_37.pdf.
25. Khalafallah, O., Total solar radiation and ideal incline angles of a south-facing solar panel in Qena/Egypt, *Resour. Environ.,* 2020, vol. 10, no. 1, pp. 10–17. https://doi.org/10.5923/j.re.20201001.03
26. Frimpong A., Anto, E., Ramde, E., and Mensah., L., Determination of optimum tilt angle for rooftop solar photovoltaic system installation for Kiku Kinderhaus in Kumasi, *Int. J. Energy Environ. Sci.,* 2020, vol. 5, no. 1, pp. 7–13. https://doi.org/10.11648/j.ijees.20200501.12
27. Romero, J., Garrido, D., Scoberanis, M., and Bañuelos, M., Estimation of the optimum tilt angle of solar collectors in Coatzacoalcos, Veracruz, *Renewable Energy,* 2020, vol. 153, pp. 615–623. https://doi.org/10.1016/j.renene.2020.02.045
28. Yassir, A., Zamzami, U., Fauzan, K., and Hasannuddin, T., Optimization of tilt angle for photovoltaic: Case study Sabang-Indonesia, *Int. Conf. Sci. Innovated Eng. (I-COSINE),* IOP Conf. Series: Materials Science and Engineering, 2019, vol. 536, p. 012055. https://doi.org/10.1088/1757-899X/536/1/012055
29. Daus, Y., Pavlov, A., and Yudaev, V., Increasing solar radiation flux on the surface of flat-plate solar power

plants in Kamchatka krai conditions, *Appl. Sol. Energy,* 2019, vol. 55, pp. 101–105. https://doi.org/10.3103/S0003701X19020051

30. Bobkov, V. and Elistratov, V., Simulation of photovoltaic module operation modes and tilt angle optimization according to the criterion of maximum electricity generation, *Appl. Sol. Energy,* 2021, vol. 57, pp. 233–241. https://doi.org/10.3103/S0003701X21030038
31. Abdullahi, B., Abubakar, B., Muhammad, N., Al-Dadah, R., and Mahmoud, S., Optimum tilt angle for solar collectors used in Kano, Nigeria, *J. Adv. Res. Fluid Mech. Therm. Sci.,* 2019, vol. 56, no. 1, pp. 31–42. https://www.akademiabaru.com/doc/ARFMTSV56_N1_P31_42.pdf
32. Hailu, G. and Fung, A., Optimum tilt angle and orientation of photovoltaic thermal system for application in Greater Toronto Area, Canada, *Sustainability,* 2019, vol. 11, p. 6443. https://doi.org/10.3390/su11226443
33. Rowlands, I., Kemery, B., and Morrison, I., Optimal solar-PV tilt angle and azimuth: An Ontario (Canada) case-study, *Energy Policy,* 2011, vol. 39, pp. 1397–1409. https://doi.org/10.1016/j.enpol.2010.12.012
34. Nfaoui, M. and El-Hami, K., Optimal tilt angle and orientation for solar photovoltaic arrays: Case of Settat city in Morocco, *Int. J. Ambient Energy,* 2018, vol. 41, no. 2, pp. 1–18. https://doi.org/10.1080/01430750.2018.1451375
35. Kim, G., Han, D., and Lee, Z., Solar panel tilt angle optimization using machine learning model: A case study of Daegu City, South Korea, *Energies,* 2020, vol. 13, p. 529. https://doi.org/10.3390/en13030529
36. Khorasanizadeh, H., Mohammadi, K., and Mostafaeipour, A., Establishing a diffuse solar radiation model for determining the optimum tilt angle of solar surfaces in Tabass, Iran, *Energy Convers. Manage.,* 2014, vol. 78, pp. 805–814. https://doi.org/10.1016/j.enconman.2013.11.048
37. Alelaj, F. and Alqallaf, A., Optimization of the tilt angle of the photo-voltaic module in Kuwait, *2019 IEEE 10th GCC Conference and Exhibition (GCC), Kuwait,* 2019, pp. 1–6. https://doi.org/10.1109/GCC45510.2019.1570525127
38. Al-Rawahi, Z., Zurigat, H., and Al-Azri, N., Prediction of hourly solar radiation on horizontal and inclined surfaces for Muscat/Oman, *J. Eng. Res.,* 2011, vol. 8, no. 2, pp. 19–31. https://doi.org/10.24200/tjer.vol8iss2pp19-31
39. Javed, W., Wubulikasimu, Y., Figgis, B., and Guo, B., Characterization of dust accumulated on photovoltaic panels in Doha, Qatar, *Sol. Energy,* 2017, vol. 142, pp. 123–135. https://doi.org/10.1016/j.solener.2016.11.053
40. Tamimi, A. and Sowayan, A., Optimum tilt angles of flat-plate solar collectors at Riyadh, Kingdom of Saudi Arabia, *Energy Sources, Part A,* 2012, vol. 34, no. 13, pp. 1213–1221. https://doi.org/10.1080/15567036.2011.598899
41. Jafarkazemi F. and Saadabadi, S., Optimum tilt angle and orientation of solar surfaces in Abu Dhabi, UAE, *Renewable Energy,* 2013, vol. 56, pp. 44–49. https://doi.org/10.1016/j.renene.2012.10.036
42. Mraoui, A., Khelif, M., and Benyoucef, B., Optimum tilt angle of a photovoltaic system: Case study of Algiers and Ghardaia, *Proc. 5th Int. Renewable Energy Congr. (IREC),* 2014, pp. 1–6.
43. Skeiker, K., Optimum tilt angle and orientation for solar collectors in Syria, *Energy Convers. Manage.,* 2009, vol. 50, pp. 2439–2448. https://doi.org/10.1016/j.enconman.2009.05.031
44. Abdallah, R., Juaidi, A., Abdel-Fattah, S., and Agugliaro, F., Estimating the optimum tilt angles for south-facing surfaces in Palestine, *Energies,* 2020, vol. 13, p. 623. https://doi.org/10.3390/en13030623
45. Bailek, N., Bouchouicha, K., Aoun, N., EL-Shimy, M., Jamil, B., and Mostafaeipour, A., Optimized fixed tilt for incident solar energy maximization on flat surfaces located in the Algerian Big South, *Sustainable Energy Technol. Assess.,* 2018, vol. 28, pp. 96–102. https://doi.org/10.1016/j.seta.2018.06.002
46. Şahin, M., Determining optimum tilt angles of photovoltaic panels by using artificial neural networks in Turkey, *Tech. Gazette,* 2016, vol. 26, no. 3, pp. 596–602. https://doi.org/10.17559/TV-20160702220418
47. Hassan, Z., Al Garni, A., and Wright, D., Optimal orientation angles for maximizing energy yield for solar PV in Saudi Arabia, *Renewable Energy,* 2019, vol. 133, pp. 538–550. https://doi.org/10.1016/j.renene.2018.10.048
48. Kaddoura, T., Ramli, M., and Al-Turki, Y., On the estimation of the optimum tilt angle of PV panel in Saudi Arabia, *Renewable Sustainable Energy Rev.,* 2016, vol. 65, pp. 626–634. https://doi.org/10.1016/j.rser.2016.07.032
49. Abdeen, E., Orabi, M., and Hasaneen, E., Optimum tilt angle for photovoltaic system in desert environment, *Sol. Energy,* 2017, vol. 155, pp. 267–280. https://doi.org/10.1016/j.solener.2017.06.031
50. Kallioğlu, M., Durmuş, A., Karakaya, H., and Yılmaz, A., Empirical calculation of the optimal tilt angle for solar collectors in northern hemisphere, *Energy Sources, Part A,* 2019, vol. 42, no. 11. https://doi.org/10.1080/15567036.2019.1663315
51. Jacobson, M. and Jadhav, V., World estimates of PV optimal tilt angles and ratios of sunlight incident upon tilted and tracked PV panels relative to horizontal panels, *Sol. Energy,* 2018, vol. 169, pp. 55–66. https://doi.org/10.1016/j.solener.2018.04.030
52. Stanciu, C. and Stanciu, D., Optimum tilt angle for flat plate collectors all over the World—A declination dependence formula and comparisons of three solar radiation models, *Energy Convers. Manage.,* 2014, vol. 81, pp. 133–143. https://doi.org/10.1016/j.enconman.2014.02.016
53. Abdulsalam, H. and Alibaba, H., Optimum tilt angle for photovoltaic panels in Famagusta, Cyprus, *Int. J. Soc. Sci. Humanit. Res.,* 2019, vol. 7, pp. 29–35. https://researchpublish.com//upload/book/Optimum%20Tilt%20Angle-6954.pdf.

54. Nassar, Y., Hafez, A., and Alsadi, Y., Multi-factorial comparison for 24 distinct transposition models for inclined surface solar irradiance computation in the state of Palestine: A case study, *Front. Energy Res.,* 2020, vol. 7, p. 163. https://doi.org/10.3389/fenrg.2019.00163
55. JS Solar. https://www.jssolar.com/en/panel.
56. Fortunes Solar. https://www.fortunes-solar.com/solar-panel/.
57. ENF Solar. https://www.enfsolar.com/directory/panel.
58. Taye, B. and Workineh, T., GIS-based irrigation dams potential assessment of floating solar PV system, *J. Energy,* 2020, vol. 2020, p. 1268493. https://doi.org/10.1155/2020/1268493
59. Alsadi, S. and Nassar, Y., A numerical simulation of a stationary solar field augmented by plane reflectors: Optimum design parameters, *Smart Grid Renewable Energy,* 2017, vol. 8, pp. 221–239. https://doi.org/10.4236/sgre.2017.87015
60. Alsadi, S. and Nassar, Y., Estimation of solar irradiance on solar fields: An analytical approach and experimental results, *IEEE Trans. Sustainable Energy,* 2017, vol. 8, no. 4, pp. 1601–1608. https://doi.org/10.1109/TSTE.2017.2697913
61. Nassar, Y., Alsadi, S., El-Khozondar, H., and Refaat, S., Determination of the most accurate horizontal to tilted sky-diffuse solar irradiation transposition model for the capital cities in MENA region, *3rd International Conference on Smart Grid and Renewable Energy (SGRE),* Doha, Dubai, March, 22–24, 2022. https://doi.org/10.1109/SGRE53517.2022.9774146
62. NIST Engineering Statistics Handbook. 4.6.3.4 Weighting to Improve Fit. https://www.itl.nist.gov/div898/handbook/pmd/section6/pmd634.htm.
63. Stone, R., Improved statistical procedure for the evaluation of solar radiation estimation models, *Sol. Energy,* 1993, vol. 51, no. 4, pp. 289–291.
64. Alsadi, S. and Nassar, Y., Correction of the ASHRAE clear sky model parameters based on solar radiation measurements in the Arabic countries, *Int. J. Renewable Energy Technol. Res.,* 2016, vol. 5, no. 4, pp. 1–16. https://scholar.ptuk.edu.ps/handle/123456789/210.